

promoting access to White Rose research papers



Universities of Leeds, Sheffield and York
<http://eprints.whiterose.ac.uk/>

This is an author produced version of a paper to be/subsequently published in Steel Research International.

White Rose Research Online URL for this paper:
<http://eprints.whiterose.ac.uk/4691>

Published paper

Kirkwood, D.H. and Ward, P.J. (2004), *Numerical Modeling of Semisolid Flow under Processing Conditions*, Steel Research International, Volume 75: 8/9, 519-524,

Numerical Modeling of Semisolid Flow under Processing Conditions

D.H.Kirkwood and P.J Ward

Dept. of Engineering Materials,
University of Sheffield, Sheffield S1 3JD, UK

Abstract

During the industrial process of Semisolid Forming (or Thixoforming) of alloy slurries, typically the operation of die filling takes around 0.1s. During this time period the alloy slug is transformed from a solid-like structure capable of maintaining its shape, into a liquid-like slurry able to fill a complex die cavity: this involves a decrease in viscosity of some 6 orders of magnitude. Many attempts to measure thixotropic breakdown experimentally in alloy slurries have relied on the use of concentric cylindrical viscometers in which viscosity changes have been followed after shear rate changes over times above 1s to in excess of 1000s, which have little relevance to actual processing conditions and therefore to modeling of flow in industrial practice. The present paper is an attempt to abstract thixotropic breakdown rates from rapid compression tests between parallel plates moving together at velocities of around 1m/s, similar to industrial conditions. From this analysis, a model of slurry flow has been developed in which rapid thixotropic breakdown of the slurry occurs at high shear rates.

Keywords: semisolid alloys, thixotropy, flow modelling

Introduction

Die design for conventional die-casting has in the past been largely a matter of accumulated practical experience together with preliminary testing and adjustment, examining the diecast product to eliminate defects such as short runs, laps, porosity etc. This is an expensive procedure both in time and cash, and computer modeling of the process has been developed by many operators to reduce or eliminate it. In semisolid processing (thixoforming), the problem of modeling is made more difficult by the non-Newtonian viscosity encountered as shearing of the semisolid alloy slurry breaks down the internal structure, leading to lower viscosities with time during the filling operation which is not uniform throughout the system. The problem is further complicated by additional solidification occurring during filling: this has been ignored in the present analysis since this is assumed to be very small at this stage because of rapid filling. A further limitation in our model is the assumption that the slurry behaves as a homogeneous material, which may be described by a single viscosity at any point. This restricts considerations to those of rapid shear and to fraction solids of less than 0.6, well within the conditions of normal thixoforming.

A typical situation is that of a semisolid slug of length 100mm being injected into a die by a ram moving at 1m/s, taking therefore 0.1s to fill the cavity. In this time the slug changes from being essentially solid-like able to sustain its shape, to being liquid-like able to flow within a complex shaped die cavity and to fill the shape. This requires a change of viscosity from around 10^6 Pa.s to 1Pa.s. Most existing rotational viscometers are unable to follow rapid shear changes of this magnitude; in general, the shear rate change measurements takes place over several seconds, although results have been recorded recently [1] from step jumps occurring in 0.15s. However these jumps have not been obtained from the stiff state of a newly formed semisolid slug, and do not represent the breakdown conditions experienced in industrial

thixotropy. Many early attempts to model the flow of thixotropic semisolid alloys employed single breakdown coefficients [2,3], independent of shear rate, and frequently derived from shear rate jump experiments conducted over 30 min to achieve steady state conditions.

The first attempt to approach industrial conditions of rapid shear rate changes was the work of Loué et al.[4] in measuring viscosities over a large range of shear rates from 10^{-3} to 10^{+3} s^{-1} , using parallel plate compression for slow shear rates and back extrusion experiments for high shear rates. Rapid compression experiments between parallel plates have been carried out by Kapranos[5] and Liu et al.[6], and in drop forging experiments by Yurko and Flemings [7], both of which have generated viscosity data under rapid shearing conditions using a Stefan analysis assuming only radial flow between the plates. However this information has not been integrated into a complete thixotropic model capable of simulating slurry flow into a die. The construction of such a model from existing experimental data is the object of the present paper.

Yield Points

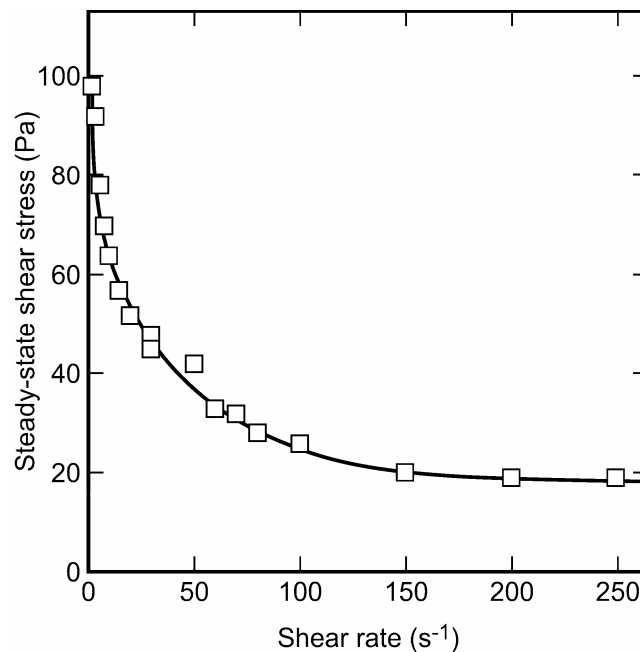


Figure 1 Steady state shear stress σ as a function shear rate in Sn-Pb alloy [10]

A number of models are based on Herschel-Bulkley flow incorporating a yield stress determined from the extrapolation of flow stress measurements at intermediate shear rates down to 20 s^{-1} [8]. Other experiments [1,4,9,10] conducted at much lower shear rates contradict this assumption of a limiting value of stress (see Fig.1), and demonstrate that at steady state the viscosity and shear stress continue to increase with decreasing stress, and the complete range of shear rates may be described adequately by the Cross (or Carreau) equation (see Fig.2). Barnes [11] has also disputed the existence of yield points in rheology and has suggested they are in fact the

consequence of instrumental inadequacy. If there is no compelling evidence for a yield point as a constant value of stress as flow is reduced, the question then arises of the usefulness of this concept in any practical engineering sense. One argument against it is that it is unnecessary, and requires a complex algorithm to include it within a computer program. A more serious objection is that a yield stress in principle acts instantaneously both as the stress is increased and decreased, and produces in the slurry regions described as ‘unyielded’ or dead [12]. We know however that shear-thinned slurries take much longer times to ‘thicken’ than die injection times, and this could provide a misleading model of die filling. So that from a practical as well as a theoretical view point, the employment of a yield point concept should be avoided. Having said this however, there is a unique condition associated with the start of structural breakdown (see Fig.3) where a maximum stress may occur at around 10kPa, and this may be taken to be the yield point as seen in compression tests, due to the breakdown of a solid skeletal structure. However this is of a different magnitude from that proposed in the Herschel-Bulkley modelling.

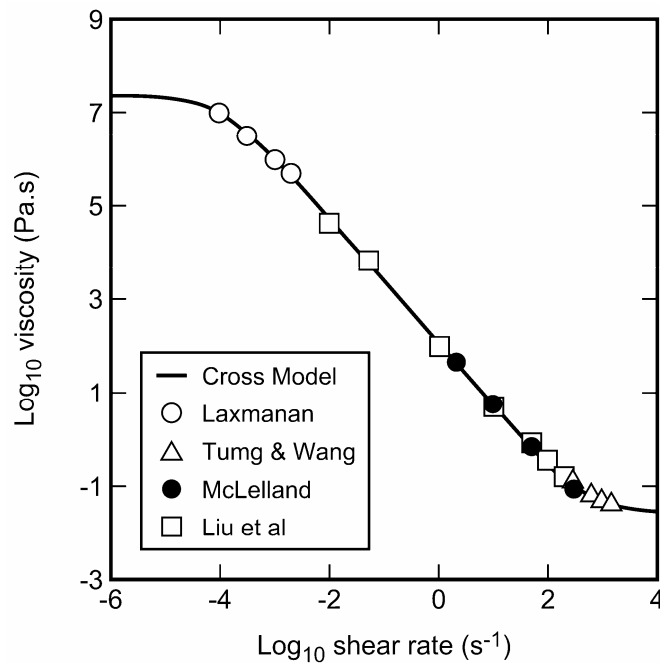


Figure 2. Equilibrium viscosity as a function of shear rate in Sn-Pb alloy, $f_s=0.36$, fitted to Cross Model.

Two-Stage Structural Breakdown

It was observed by Martin et al [13] using a cylindrical rheometer and fast data capture (1Hz) that, during rapid shear rate jumps, a decrease in shear stress initially occurred very rapidly followed by a slower decay to the steady state value. Later the same phenomenon was observed by Quaak et al.[14] working on Al-Si alloys, both in up and down shear rate jumps, which they analysed as two exponentially varying processes:

$\sigma - \sigma_e = (\sigma_i - \sigma_e)[\alpha e^{-t/\tau_1} + (1 - \alpha)e^{-t/\tau_2}]$, where α is the partitioning of the overall shear stress between the two processes. The relaxation time of the first stage τ_1 in an up-jump was of the order of 1s or less, and was attributed to the break up of agglomerates into smaller units under the action of hydrodynamic shear stresses. Whereas the second stage τ_2 occurred over minutes and involved the slower processes

of spheroidisation and coarsening by diffusion. It seems clear that only the first stage is involved in industrial thixoforming.

Liu et al.[1] have examined these processes in greater detail in Sn-Pb semisolid slurries, taking account of inertial effects of the rheometer and using rapid data capture.

Kinetics Of Structural Breakdown In Thixotropic Semi-solid Slurries

Following Cheng [15], we assume a simple expression as an equation of state:

$$\eta = \eta_{\infty} + c\lambda \quad (1)$$

where the apparent viscosity η of a semisolid slurry is linearly related to its internal structure λ , whose value is zero for the fully broken down condition as $\dot{\gamma}$, the shear rate, becomes large (i.e. it consists of free discrete solid particles dispersed in a liquid matrix) and unity in the fully built up condition developed as $\dot{\gamma}$ approaches zero (i.e. large interlocking agglomerates). Under these conditions, the value of the constant, c , is given by $\eta_0 - \eta_{\infty}$, where η_0 is the asymptotic viscosity at low shear rates and η_{∞} that at high shear rates. It should be noted that in this simple model, the structural parameter λ is defined as: $(\eta - \eta_{\infty}) / (\eta_0 - \eta_{\infty})$ and is therefore a linear function of viscosity η .

We now introduce a generalised kinetic equation for structural change [13,15]:

$$\frac{d\lambda}{dt} = a(1 - x\lambda) - b\lambda \dot{\gamma}^m \quad (2)$$

where the first term on the right hand side describes the rate of structural build up being proportional to the extent of unbuilt-up structure. The second term describes the rate of breakdown proportional to the degree to which structure is already built up, and to the magnitude of the shear rate. Equilibrium is achieved at $d\lambda/dt=0$, leading to $a = \lambda_e(ax + b\dot{\gamma}^m)$ and $\lambda_e = 1 / (x + (b/a)\dot{\gamma}^m)$. Hence, $\eta_e = \eta_{\infty} + (\eta_0 - \eta_{\infty}) / (1 + (b/a)\dot{\gamma}^m)$ when $x=1$; this is the Cross steady state equation. When $x=0$, we obtain the Sisko equation [16].

The assumption implicit in eqn.1 is that for constant λ , η is also constant (i.e. Newtonian) and therefore isostructural curves on a σ v. $\dot{\gamma}$ diagram (Cheng diagram) are straight lines passing through the origin, as shown in Fig.3. The slope of the $\lambda=1$ curve is η_0 , and of $\lambda=0$ is η_{∞} in the Cross equation above. The steady state Cross equation is represented by the curve crossing the isostructural lines as indicated showing a breakdown in structure. Where a maximum stress occurs at the beginning of structural breakdown (A) at low shear rate, this may be identified with the peak frequently observed in compression tests. It should be noted that the above assumption of Newtonian isostructural flow has been challenged by Martin et al.[13] who believed it to exhibit shear thickening. However this conclusion has not been supported by the work of de Figueredo et al.[17], and furthermore the theoretical

modeling by Chen and Fan [18,19] indicates that the viscosity at constant structure is not dependent on shear rate.

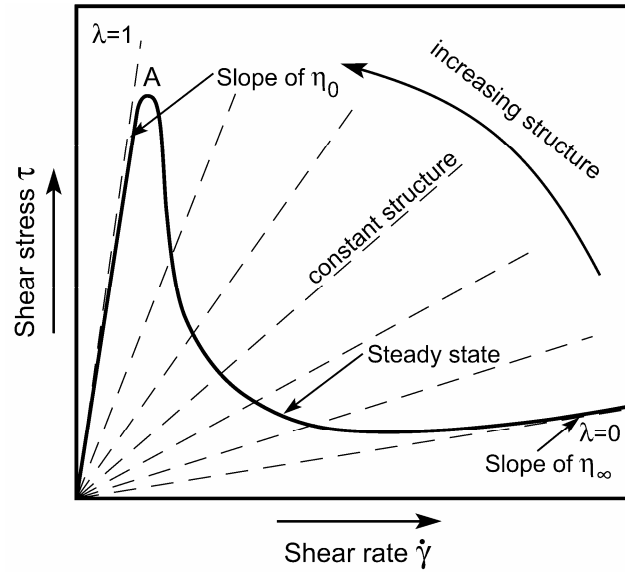


Figure 3. Cheng Diagram: shear stress vs. shear rate

It may also be demonstrated by substituting for a in eqn.2 and noting that $\eta \propto \lambda$ from eqn.1, that $d\eta/dt = (a + b\dot{\gamma}^m)(\eta_e - \eta)$. This is the expression used to calculate viscosity changes in the present work.

If the slurry suffers a step change in shear rate, we may integrate the above kinetic equation assuming a new constant shear rate $\dot{\gamma}$ to obtain:

$$(\lambda - \lambda_e) / (\lambda_i - \lambda_e) = \exp(-(a + b\dot{\gamma}^m)t) \quad (3)$$

Since λ is proportional to the viscosity, which in turn is proportional to the shear stress σ , we have $\sigma - \sigma_e = (\sigma_i - \sigma_e) \exp(-(a + b\dot{\gamma}^m)t)$, showing that at constant shear rate the shear stress decays exponentially to the steady-state stress σ_e from a value of σ_i at $t=0$. This will provide a characteristic decay time τ such that:

$$\tau = 1 / (a + b\dot{\gamma}^m) \quad (4)$$

The above analysis assumes a single stage process leading to the steady-state conditions. However, as has been noted above, Quak et al.[14] have shown that this is incorrect and at least two processes are involved in a shear rate increase: a very rapid process believed to involve the disruption of the agglomerates into smaller pieces under the increased shear stresses, and a slower process involving their spheroidisation leading to the true steady-state condition. The latter taking some minutes has frequently been measured, but it is the former, taking place in a fraction of a second, which is actually of interest in commercial semisolid processing. We have made the assumption in the present work that rapid breakdown leading to a partial or pseudo steady-state condition, can also be described by the kinetic equation given above, having an exponential shear stress decay to the pseudo steady-state with a characteristic or relaxation time τ of the same form.

Previous Work

Recent work by Liu et al. [1,6] has investigated the response of semisolid alloy Sn-Pb slurries to rapid shear rate changes in a Searle type viscometer and the rapid compression of semisolid Al alloys under conditions similar to industrial thixoforming.

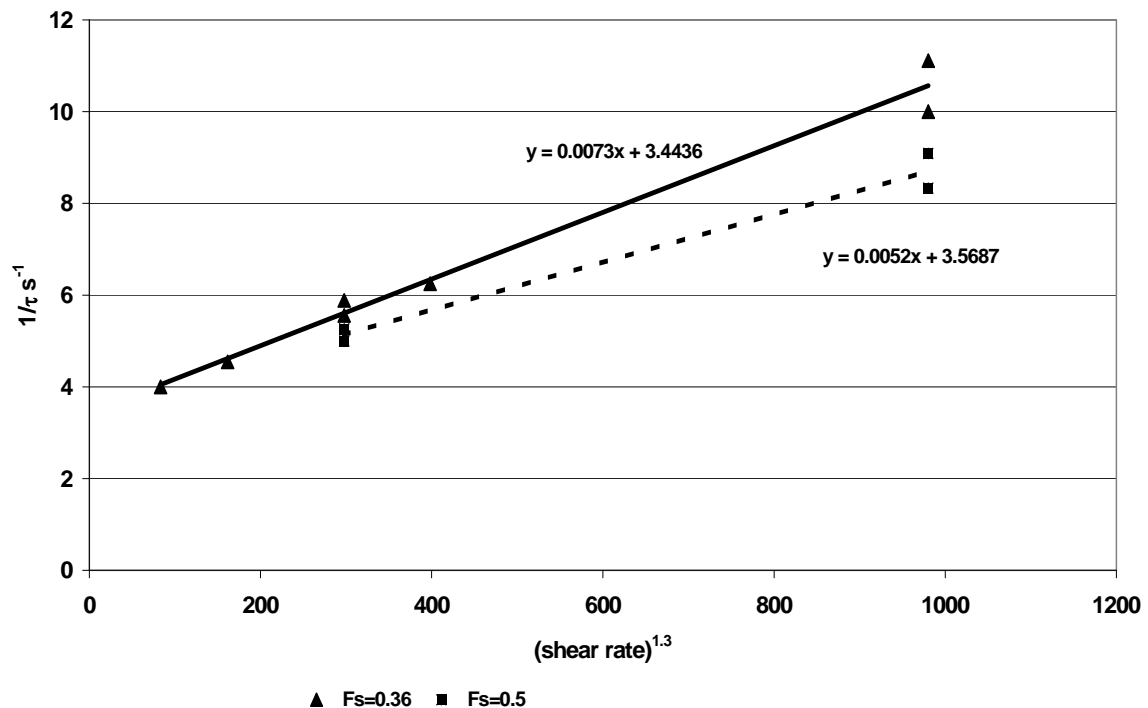


Figure 4. Reciprocal of experimental breakdown time vs. $\dot{\gamma}^{1.3}$ for Sn-Pb.

The viscometer results [1] on shear rate jumps between 1 and 200s⁻¹, demonstrated that the kinetics of structural change was dependent only on the final shear rate and not on the initial rate. Figure 4 shows that plotting $1/\tau$ against $\dot{\gamma}^{1.3}$ produces a definite linear relationship for the Sn alloy containing 0.36 fraction solid, in agreement with theoretical expectation (equation 4), using a value of m derived from steady-state measurements. A similar relationship is found for 0.5 fraction solid although with fewer data points because of the experimental difficulties in the stiffer alloy system. Plotting the value of τ against $\dot{\gamma}$ (Figure 5) indicates that for the relaxation time to be comparable to a processing time of around 0.1s, the shear rate must exceed 200s⁻¹ and that above 1000s⁻¹ the value of τ falls dramatically.

The second piece of work employing rapid compression [6] showed the effects of temperature, soaking time and ram velocity on the force exerted on a cylindrical slug of semisolid Al alloy (A356) by a ram moving at a nominally constant velocity. The results showed an initial peak in the force/displacement curve, which is believed to be associated with the breakdown of a solid skeleton structure existing within the slurry (point A in Fig.3). This peak falls with increasing temperature and with soaking time as the skeletal structure is destroyed until at the highest temperature (581°C) at which commercial thixoforming is carried out it is barely apparent. Following the peak, the force drops to a minimum where slurry flow begins, before rising as the slug height falls and the shear rate between the moving platens increases.

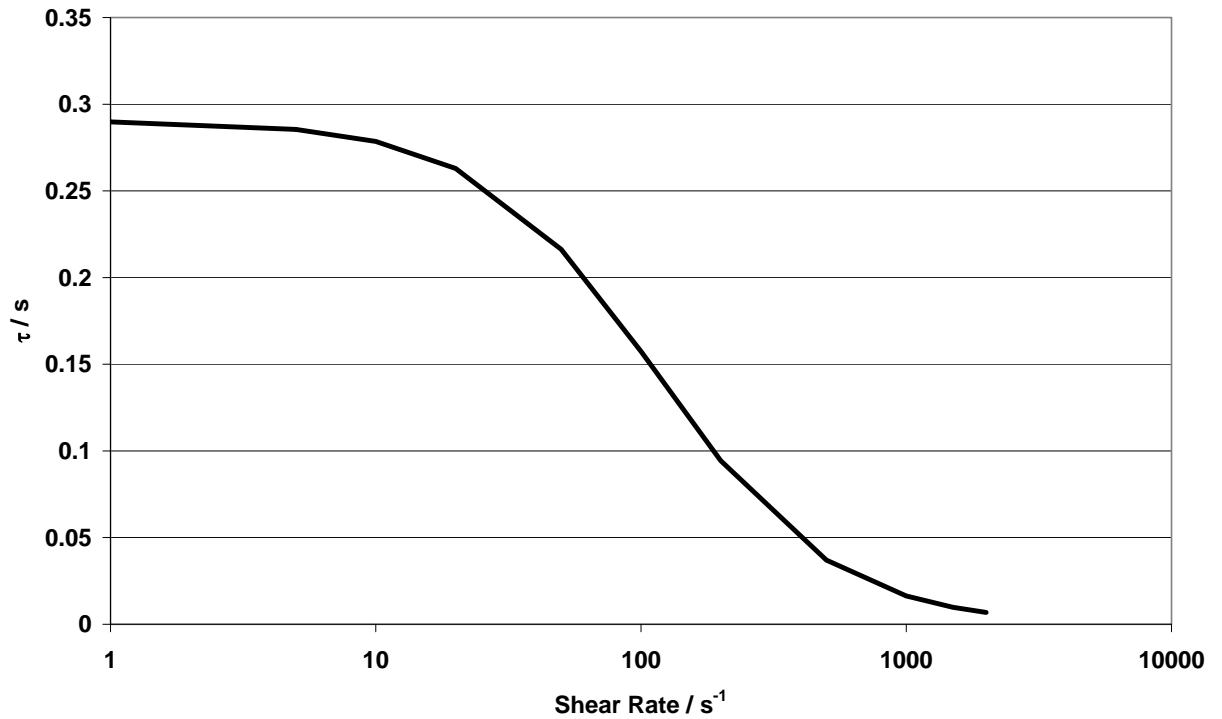
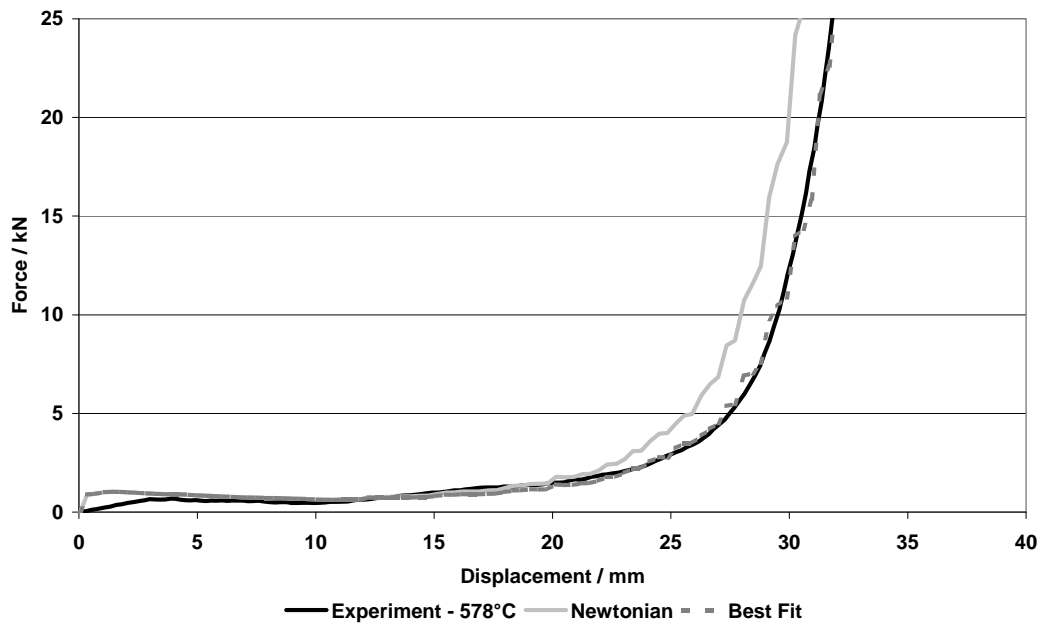
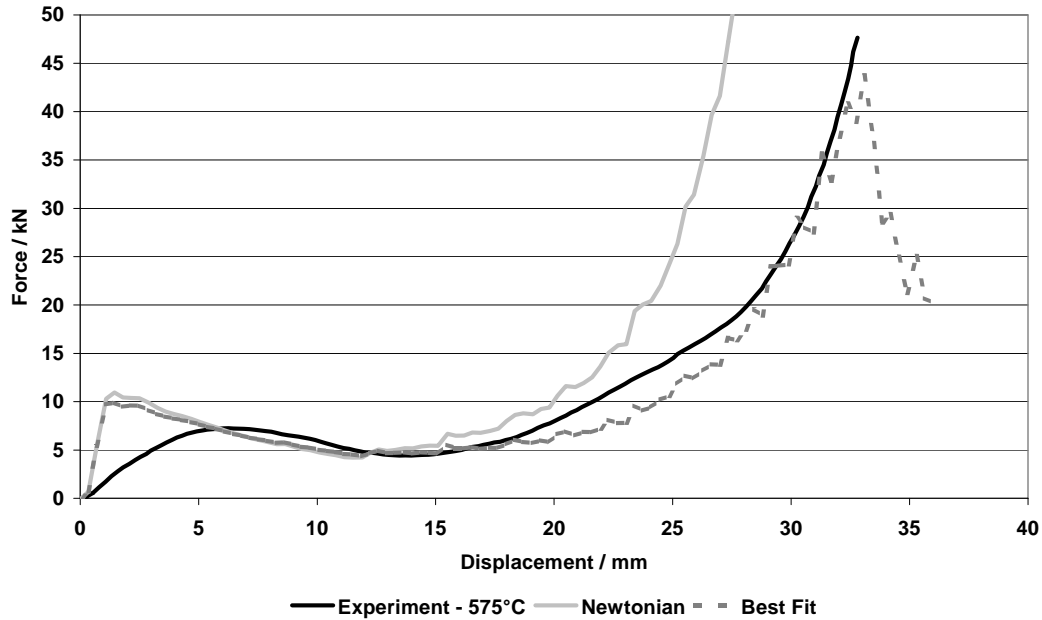


Figure 5. Relaxation time, τ , as a function of shear rate. From Figure 4.

We have attempted to simulate these force/displacement curves by assuming that two successive processes in the rapid compression experiments: the breakdown of a skeletal structure followed by the flow of a slurry consisting of separate agglomerate particles. The former might be considered to be a weak solid having a yield stress and yield strain, or it can be modeled as a stiff liquid of high viscosity. For reasons associated with computational ease, we have chosen the second approach but this does not imply any preference as to the true nature of the slurry at this stage.

Initially we used the Stefan [9] equation which assumes only radial flow during compression of the cylindrical slug, supplying an initial viscosity η_1 and relaxation time τ_1 to fit the peak stage of the process to which was added a second lower viscosity having a longer breakdown time τ_2 to simulate the subsequent flow of the



Figures 6a and 6b. Experimental and modelled results for compression test on Al-A356 alloy at two temperatures.

slurry. It was possible to obtain a reasonable agreement with experiment by adjusting these four parameters. However when these data were fed into the more powerful and realistic FLOW-3D® program of FlowScience (which in particular allows for axial flow as well as radial flow of the cylinder), it produced forces 10 times larger than the Stefan predictions, and we have concentrated therefore on using only FLOW-3D to obtain the rheological data from the simulation exercise.

In the present version of FLOW-3D® (version 8.2) it is possible to assign only one value of viscosity to each computational cell and we could not follow the original procedure of summing two viscosities appropriate to the two processes. The strategy adopted therefore was to assign an initial viscosity and breakdown time to simulate the peak, and then to reassign a new breakdown rate to simulate the flow stage on achieving a specified viscosity (the switch viscosity) in each cell. Also given the shear rate sensitivity of the breakdown rate observed in Sn alloys [1], we have incorporated a term from the empirical equation derived from Figure 1 above, which is unlikely to contribute much to the breakdown time below $\dot{\gamma}=100\text{s}^{-1}$.

The effect of temperature on the experimental flow curves (force v. displacement) is shown for 575°C and 578°C in Figures 3a and b. In generating the computer simulation curve, the force has been made to coincide at the minimum where true flow is judged to start by adjusting the viscosity at this point. It is clear from these figures, Newtonian (constant viscosity) conditions do not obtain, since the experimental flow curves always lie below them, indicating that structural breakdown is occurring and the viscosity is decreasing. By adjusting the values of a and b in the rate equation, the best fit with experiment is obtained and these values have been recorded in the Table 1. It is seen that $a=10 \text{ s}^{-1}$ (equivalent to a characteristic breakdown time τ of 0.1s) satisfies the earlier part of the curve, but agreement is further improved by including some shear rate sensitivity as b , particularly at the lower temperature affecting the force at higher shear rates.

Similar best fit simulation curves have been obtained [20] for other conditions, such as soaking times up to 5min at 575°C and different compression velocities. Table 1 records the best fit values of a and b in the rate equation.

Experiment	Conditions	a	b	switch viscosity, Pa.s
Effect of Temperature (500 mm/s)	575°C	10	0.24	9×10^4
	576°C	10	0.14	3.5×10^4
	578°C	10	0.03	3.5×10^4
Effect of Soak Time (500 mm/s)	0 min soak	10	0.05	1.8×10^4
	5 min soak	1	0.05	9×10^3
Effect of Velocity (576°C)	350 mm/s	10	0.037	1.8×10^4
	500 mm/s	22.2	0.037	1.8×10^4
	1000 mm/s	22.2	0.07	5×10^3

The work of Yurko and Flemings

There are few experiments containing quantitative information in the literature, which may be used to test the above thixotropic model for shear thinning. Recently Yurko and Flemings [7] have employed a drop-forge viscometer on short A357 aluminum billets, to obtain shear rates up to 1300s^{-1} and viscosities as a function of time determined from the Stefan equation using the instantaneous compression velocity. The volume-averaged viscosity and shear rate are reproduced in Fig.7 showing a rapid

drop to 6 Pa.s in about 4ms at a shear rate of 800s^{-1} ; furthermore, as the shear rate decreases thereafter, the low viscosity is maintained. This has important practical consequences allowing fluid slurry to fill the die completely in the later stages of injection. These authors also showed that using a greater forging mass, even higher shear rates were obtained resulting in viscosities as low as 1 Pa.s without any rapid recovery.

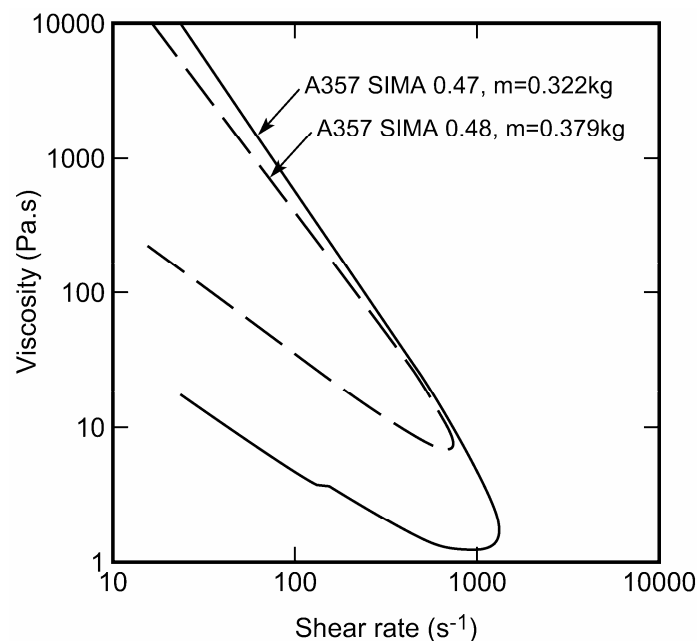


Figure 7. Drop-forge results from Yurko and Flemings [7]

In an attempt to simulate this behaviour, we have imposed their compression rate (experiment 2) on a billet of the same dimensions, using breakdown parameters similar to the values in Table1 ($a=20$, $b=0.3$). The results using FLOW-3D® indicate that shear rates are extremely non-uniform, both through the billet thickness and along the radius. This in turn severely affects the breakdown rates and local viscosity. We have therefore confined the recorded results to points initially at the mid-radius of the billet and 3 positions across the thickness (or height), including the surface and center. It is to be seen in Fig 8, on plotting viscosity as a function of shear rate that very high shear rates are achieved at the surface (over 2000s^{-1}) in about 4ms as in Yurko and Flemings [7] leading to a low viscosity, which is maintained as the shear rate subsequently falls. This effect is also seen in the central region of the billet but to a lesser extent. At the edge of the billet however very much higher shear rates occur (4500s^{-1}), corresponding to a viscosity of 3×10^{-2} Pa.s. No attempt has been made to adjust the thinning parameters to obtain a better fit with experiment, but it is clear that a lower value for b would improve the fit. This variation confirms the inadequacy of the Stefan solution even for short height billets and the need for computer analysis to deal with more complex geometries. Nevertheless the model corroborates the essential message of Yurko and Flemings that the shear-thinned slurries maintain their fluidity even after the shear rate falls. According to the present model this is a consequence of the build-up kinetics, as well as the breakdown kinetics, being very sensitive to shear rate, and when the shear rate decreases in an already shear-thinned

slurry, the shear thickening becomes slow – essentially ‘quenching in’ the shear-thinned structure.

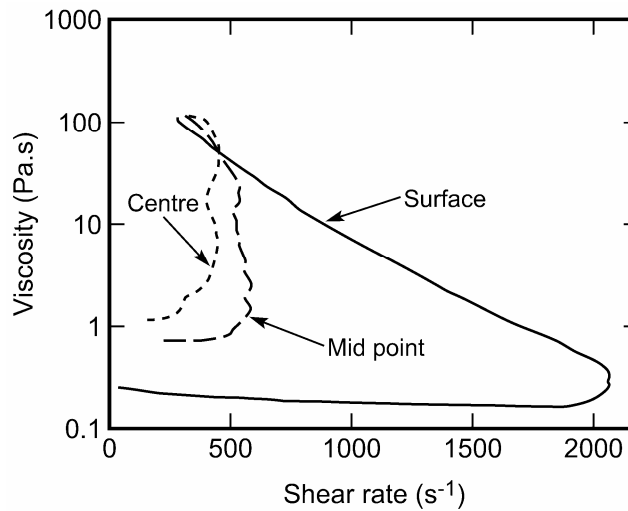


Figure 8. Prediction of FLOW-3D®

Discussion

In a previous paper [5] we performed a similar analysis on an A357 alloy, using a constant breakdown rate, independent of shear rate, and obtained a reasonably good fit with experiment at $a=20 \text{ s}^{-1}$ (or $\tau=0.05\text{s}$). Given the difficulty in obtaining precise experimental values due to their sensitivity to both temperature and soaking time, and being a different alloy, this earlier value is not too dissimilar to the present values. In fact taking into account the shear rate term b from the present analysis, the values of τ are identical at $\dot{\gamma}=100\text{s}^{-1}$. However the shear rate dependency becomes very dominant above 100s^{-1} , providing a dramatic drop in viscosity at higher shear rates. This has been made evident in our shear rate jump experiments [1], but was also shown very clearly in the work of Yurko and Flemings [7] using a drop forge viscometer. They have achieved very high average strain rates up to 1330s^{-1} , reducing the viscosity to $\sim 1\text{Pa.s}$ in less than 10ms. The change in viscosity with increasing shear rate is extremely rapid towards the end of compression, where the shear rate is approaching the maximum and can only be explained by a shear rate dependent breakdown rate of the form suggested in this paper. We have attempted to simulate their experimental conditions employing reasonable values of a and b and have also demonstrated a rapid fall in viscosity, as well as the slow rate of recovery, as observed by Yurko and Flemings. This effect may easily be explained in terms of the shear rate dependency of the structural kinetics, since the build up of structure now occurs in the lower shear rate region in which the kinetics (in both directions) become much lower.

The present breakdown model relies on experimental data gathered during a period up to 1s after the shear jump. It is believed that the measured viscosity changes due to rapid structural breakdown (or build-up) are those appropriate to commercial thixoforging occurring within $\sim 0.1\text{s}$. Modigell and Koke[8] have measured transient viscosity changes occurring over several minutes, which we believe to be the effect of a second process [14] involving the spheroidisation of the newly formed

agglomerates. This process leads to the true steady-state condition that is not considered relevant to rapid thixoforming.

There is a clear need for more reliable data on the rapid breakdown and build-up kinetics of slurries having fraction solids between 0.5 and 0.6, using high torque cylindrical viscometers capable of ultra rapid jumps to high shear rates, and with high data collection facility. This should provide information on the most suitable model of shear thinning and thickening, as well as the data for use in computer simulation of industrial thixoforming.

Conclusions

1. A rate equation for the thixotropic breakdown of semisolid slurries sheared at $\dot{\gamma}$ is proposed of the form: $\tau = 1/(a+b\dot{\gamma}^m)$, where τ is the characteristic time for rapid breakdown or build up to a pseudo steady state structure, and a , b and m are constants. This relationship has been confirmed experimentally by shear rate jumps in Sn-Pb alloys over a restricted range of shear rates.
2. This breakdown rate equation has been introduced into FLOW-3D® (version 8.2: FlowScience Inc.) to simulate the force-displacement curves obtained experimentally in rapid compression tests on semisolid slugs of Al-Si alloy, compressed at different temperatures after different soaking times, and at different compression velocities.
3. The results of this analysis indicate that thixotropic behaviour is involved in all cases, but after 5min soaking (as in industrial practice) the structure has broken down significantly and, initially in the low shear rate regions, the flow is close to Newtonian.
4. The rate of breakdown is postulated to increase dramatically at shear rates above 100s^{-1} . This prediction needs to be tested by further careful work at high shear rates, but seems to be supported by drop forge experiments where average shear rates up to 1300s^{-1} have been generated [7].

References

1. T.Y.Liu, H.V.Atkinson,P.J.Ward, and D.H.Kirkwood:Metall.Mater.TransA, 33A(2003), pp409-17.
2. A.Zavaliangos and A.Lawley: J.Mater.Eng.Perform.,4(1995),40-47.
3. M.R.Barkhudarov, C.L.Bronisz, and C.W.Hirt: Proc.4th Int.Conf.on Semisolid Processing of Alloys and Composites,1996, Sheffield,p.110
4. W.R.Loué, M.Suéry, and J.L.Querbes:Proc.2ndInt.Conf.on Semisolid Processing of Alloys and Composites,1992, Cambridge MA , pp266-75.
5. P.Kapranos, D.H.Kirkwood, and M.R.Barkhudarov: Proc.5th Int.Conf.on Semisolid Processing of Alloys and Composites, Golden CO,1998, pp.11-19.
6. T.Y.Liu, H.V.Atkinson, P.Kapranos, D.H.Kirkwood and S.G.Hogg: Metall.Mater.TransA, 34A(2003), pp1545-1554.
7. J.A.Yurko and M.C.Flemings:Metall.Mater.TransA, 33A(2002), pp.2737-46.
8. M.Modigell and J.Koke: Mechanics of Time Dependent Materials,3(1999), pp15-30.
9. V.Laxmanan and M.C.Flemings: Metall.TransA, 11A(1980), pp.1927-36

10. A.R.A McLelland, N.G.Henderson, H.V.Atkinson, and D.H.Kirkwood: Mater.Sci.Eng.,A232(1997),110-118.
11. H.A.Barnes:J.Non-Newtonian Fluid Mech.,81(1999),133-178.
12. A.N.Alexandrou, E.Duc and V.Entov: J.Non-Newtonian Fluid Mech., 96(2001), 383-403.
13. C.L.Martin, P.Kumar and S.Brown:Acta Mat.Mater.,42(1994), 3603-3614.
14. C.Quaak, L.Katgerman and W.H.Kool: Proc.4thConf.on Semisolid Processing of Alloys and Composites, 1996, Sheffield, pp.35-39
15. D.C-H.Cheng: Int.Journal Cosmetic Science, 9(1987), pp.151-191.
16. An Introduction to Rheology: H.A.Barnes, J.F.Hutton and K Walters, Elsevier, Amsterdam, 1989.
17. A.M.de Figueredo, A.Kato and M.C.Flemings:Proc.6th Int.Conf.on Semisolid Processing of Alloys and Composites,2000, Turin, 477-482.
18. J.Y.Chen and Z.Fan: Mater.Sci.Tech., 18(2002), 237-242.
19. Z.Fan: Int.Mater.Rev., 47(2002)No.2, 49-85.
20. D.H.Kirkwood and P.J.Ward: Proc.8th.Int.Conf.on Semisolid Processing of Alloys and Composites,2004, Cyprus. To be published.

Acknowledgements

The authors are grateful to Professor K.Ridgway for the use of the computing facilities of the Advanced Manufacturing Centre in the University of Sheffield.

Figures

1. steady state shear stress σ plotted against shear rate $\dot{\gamma}$ in Sn-Pb alloy (ref.10)
2. $\log \eta$ v $\log \dot{\gamma}$ from Ward (Cross eqn.)
3. Cheng diagram: σ v $\dot{\gamma}$
4. $1/\tau$ vs. $\dot{\gamma}^{1.3}$
5. τ vs. $\dot{\gamma}$ from Fig.4
6. a and b: Force/displacement plots, experiment [6].
7. Yurko and Fleming's results [7]
8. FLOW-3D prediction.

Table

1. Calculated parameters for the Breakdown in Compression Tests [20]